

RELATIONSHIP BETWEEN DEFECTS PRE-HEATING AND DEFECTS SIZE

Y. Xie, H. Padamsee, A. Romanenko

Cornell Laboratory for Accelerator-Based Sciences and Education,
Cornell University (CLASSE), Ithaca, NY, U.S.A.

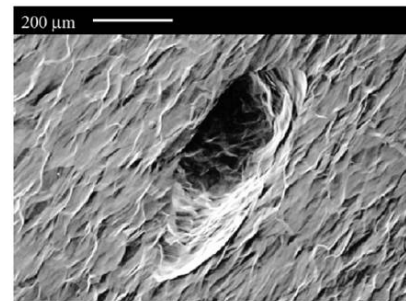
Abstract

Pit-like structures are defect candidates that cause cavity quenches. Thermometry and SEM examination results of two such pit candidates are presented. The observed and simulated correlations between defects size and pre-heating temperature near the defect region at helium side can provide useful information about the effective defect size and resistance. Calculations based on a disk-type defect model suggest that the observed pit is much larger than the actual normal conducting region responsible for initiating the quench. This finding is consistent with the sharp edge segments of the pit as the possible regions responsible.

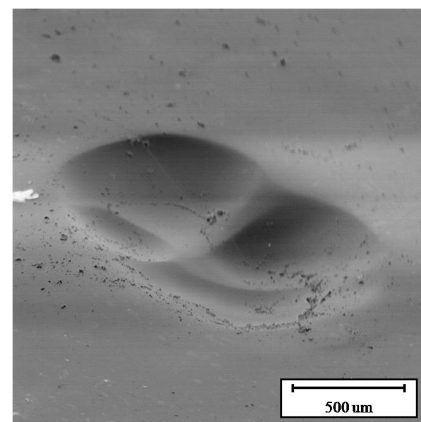
INTRODUCTION

The maximum field achieved by superconducting cavities is limited by several reasons. One of them is thermal breakdown of superconductivity caused by temperature rise initiated by a resistive or normal conducting region of sub-millimeter size. Those so-called "defect" areas were studied by both thermometry and SEM [1], [2]. Several types of defects have been thus identified [3]. Optical inspection techniques were developed and widely used to find pits or protrusions in ILC cavities [4]. Those pits or protrusions are suspected as possible defects candidates and no direct correlations between pit-like structures and defects have been established yet. Fig. 1(a) shows a pit type defect which caused thermal breakdown around 925Oe. The defect was located by thermometry. EDX analysis found no foreign elements. At the same field just below quench, the temperature map shows a 300mK pre-heating occurred at the defect area. But some of the heating was attributed to a field emitter, so the exact pre-heating due to the defect is not known. It was suspected that field enhancement at the edges of the pit created normal conducting regions which caused extra resistive heating.

Figure 1(b) is another pit-like defect found in a single cell 1.5GHz cavity which shows about 200mK pre-heating at the quench site just below the breakdown field of 1200Oe. Here some of the heating may be due to the high field Q-slope, as discussed further. Figure 2(a) is the corresponding temperature map taken just below quench field. The strongest heating area showing in the map (center, yellow) is the defect location while other less-heated areas (green) show general heating due to high-field Q slope which can be observed from the Q vs H curve of Fig. 2(b). Figure 3 is the individual thermometer response near that defect site. It shows that defect heating has surpassed high-



(a) Defect found in cavity LE1-34



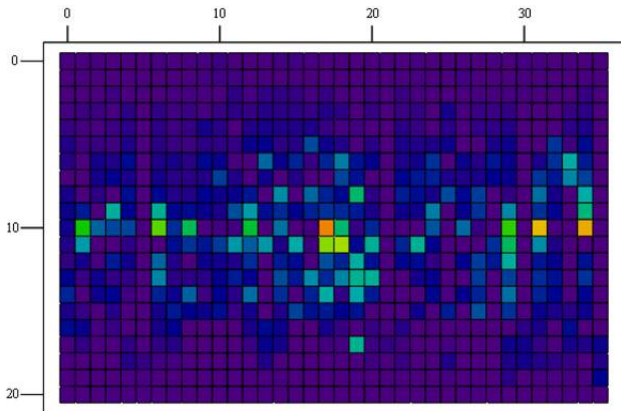
(b) Defect found in cavity LE1-HOR

Figure 1: SEM images of quench causing pits.

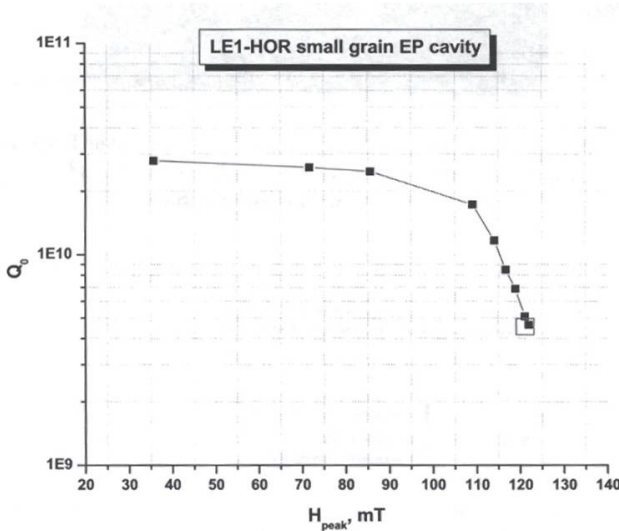
field Q slope above 800Oe. By subtracting the estimated Q slope heating, the pre-heating for defect alone is estimated about 100~180mK. The high field Q-slope heating selected is typical of the stronger heating regions in the Q-slope regime, as suggested by the strong high field Q-slope heating at the thermometers neighboring the defect. Since the thermometer efficiency is 20~25% [1], the outer wall temperature rise is 400~900mK. Thermometer efficiencies have been thoroughly calibrated as discussed in [1].

It was measured that defect heating is ohmic and temperature increases scale as H_{peak}^2 [1]. In Fig. 3, our calculations show that measured defect (pit) heating can be effectively decomposed to Q-slope heating and H_{peak}^2 ohmic heating terms.

Previous thermal model simulations predict that a normal conducting defect size such as 20μm radius will cause a quench at 1200Oe and thus would be much smaller than observed 800×600μm pit size [5]. Therefore either the active defect region is much smaller than the actual observed



(a) Temperature map at 1200Oe



(b) Q vs H

Figure 2: Q-curve and temperature map of cavity LE1-HOR.

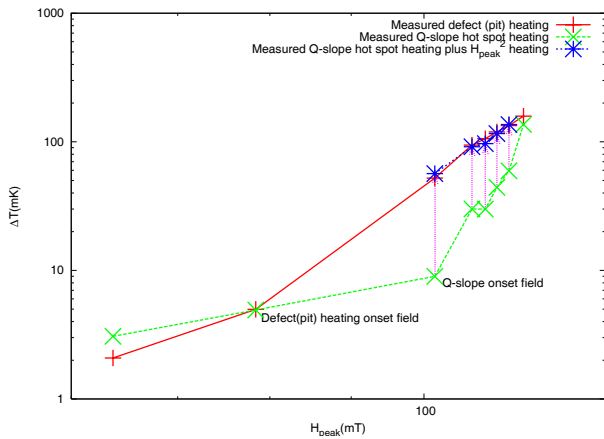


Figure 3: Individual thermometer response near defect site of cavity LE1-HOR.

pit or the effective resistance is much smaller than normal conducting niobium resistance, or some combinations of smaller defect resistance and smaller defect size cause the thermal breakdown. Since thermometry can give us temperature readings just below quench at the defect region, a calculation of the pre-heating temperature is carried out to reveal the possible size and resistance information of the quench producing area.

THERMAL FEEDBACK MODEL

The thermal program splits a cylindrical section of the niobium wall into many circular ring-shaped mesh elements. The defect is located in the center of the r.f. surface. Given the temperature dependent thermal conductivity of niobium and Kapitza conductance between niobium and helium, r.f. power produced at the surface is compared with power emitted into the helium bath for a specified iteration number. The over-relaxation method is used to guess the $(n + 1)$ -th iteration from n -th iteration. Once the two numbers are viewed as equal (e.g. their difference less than 0.1%, the temperature of those 2-d meshes are calculated as thermal equilibrium. The original program was developed by A. Deniz and H. Padamsee [6] and it was rewritten in C++ [5]. To speed up simulation and to allow some defects, the radial range is split up quartically (the width of the i -th element from the center is proportional to i^4). The z direction is also split up using an exponential function. Originally the defect resistance was taken as 10mΩ which is assumed the normal resistance of niobium.

For a specified r.f. field and defect size, the defect resistance is varied to approach thermal breakdown. The temperature distribution just below quench is obtained to show the pre-heating both at the r.f. surface and at the helium side. To check whether the quench is reached or not, the temperature around the defect at the r.f. surface should always approach $T_c(H)$. Figure 4 shows that all the calculations are approaching the thermal breakdown. The temperature T just next to the defect area is obeying:

$$T \sim T_c \sqrt{1 - \frac{H_{rf}}{H_c}} \quad (1)$$

as expected from the parabolic temperature dependence of the critical field.

To calibrate the program, we have calculated the heating due to a 50μm copper defect found on a 1.5GHz single cell cavity as a simple case [3]. We made some reasonable assumptions about the RRR and the phonon mean free path of the niobium used for the cavity. The defect was found by SEM as Fig. 5. The effective area contributed by the copper to the r.f. field is estimated from the photograph as $4 \times 10^{-9}m^2$ and thus the defect element be concluded as 35.7μm. Taken the r.f. magnetic field at the equator as 427Oe and assuming a typical copper surface resistance of 5mΩ, the power dissipated into the defect is calculated as 12.2mW. The temperature rise profile in the helium side

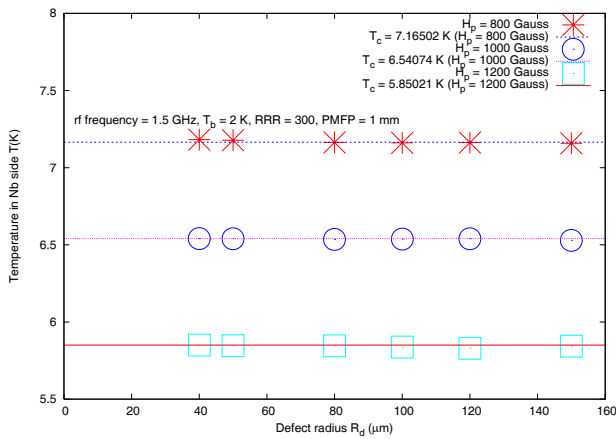


Figure 4: Calculated temperature next to defect on r.f. side near quench field.

along the axis from the defect center is shown in Fig. 6. The temperature rise near the defect is calculated as 115mK. The measured temperature rise was 39mK. Considering the thermometer efficiency of 20~25% [1], the agreement is acceptable.

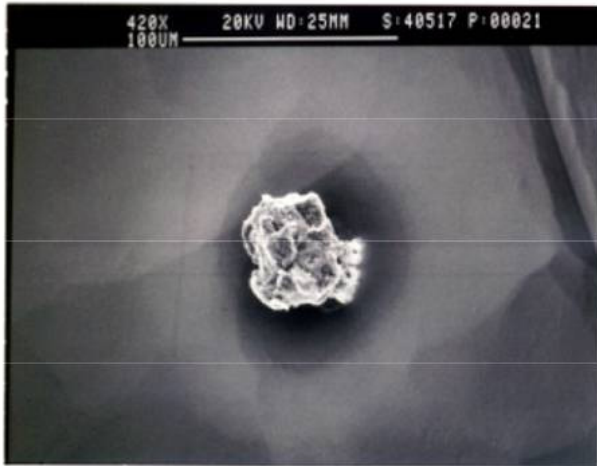


Figure 5: SEM micrograph of a defect found in a high magnetic field region of a 1.5GHz single cell cavity.

RELATIONSHIP BETWEEN DEFECT SIZE AND DEFECT PRE-HEATING

We return to the relationship between defect size, defect resistance and pre-heating. Figure 7 shows a typical pre-heating temperature distribution along the radial direction for two defect sizes under the same r.f. field. For the larger defect, the 10mΩ defect resistance has been decreased to 1mΩ to meet the same breakdown field. Although the temperature near defect area at the r.f. surface are the same in both cases as required for quench initiation, the helium side temperatures have roughly 1K difference. With a distance about several millimeters between two adjacent thermome-

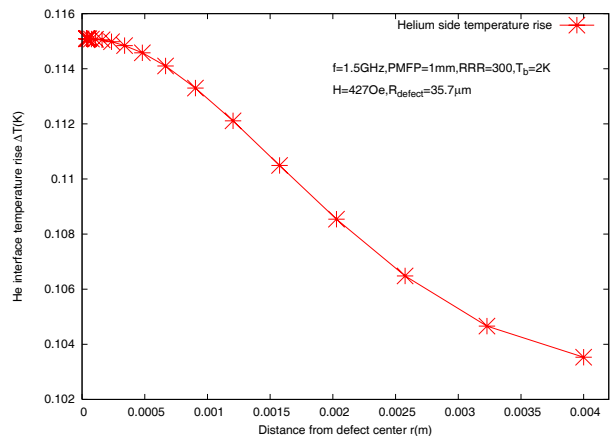
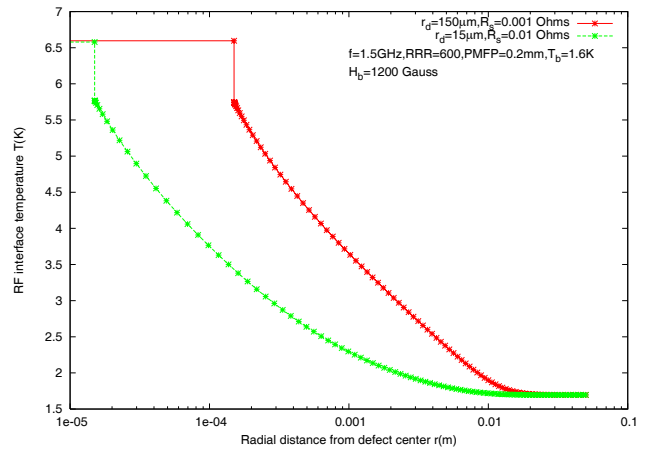
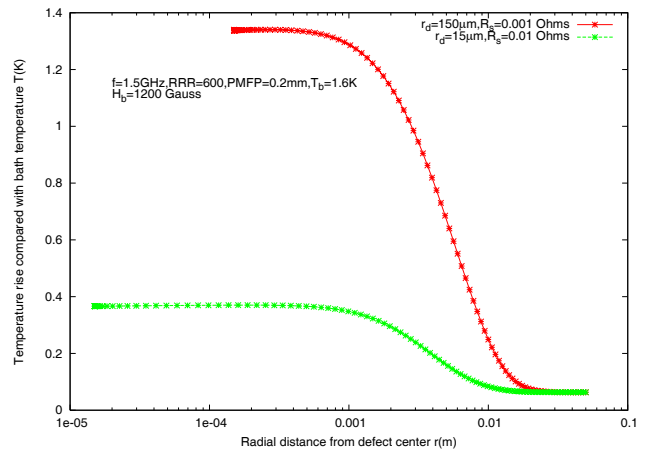


Figure 6: Helium side heating due to a copper defect.

ters, those pre-heating temperature readings can be used to get additional defect size and defect resistance information.



(a) r.f. surface temperature distribution



(b) Helium side temperature rise distribution

Figure 7: Two different size defects temperature distribution along the radial direction.

To map out the general relationship between defect size

Table 1: The resistances of different size defects

Defect sizes, μm	R_s (H=800Oe) m Ω	R_s (H=1000Oe) m Ω	R_s (H=1200Oe) m Ω
40	9.99	4.54	2.05
50	7.98	3.63	1.64
80	4.98	2.26	1.02
100	3.98	1.81	0.81
120	3.32	1.51	0.67
150	2.65	1.20	0.54

and pre-heating temperature, pre-heating temperatures for different size defects are calculated and shown in Fig. 8. The corresponding temperatures near the defect area at the r.f. surface shown in Fig. 4 indicate that all calculations are just below the quench field.

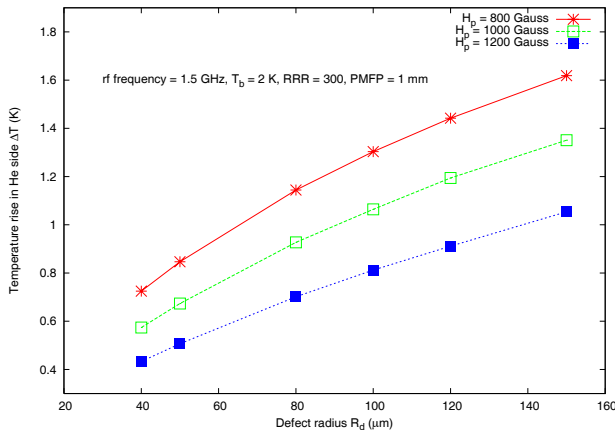


Figure 8: Different size defects with their pre-heating temperatures just near the defect spot.

Table 1 shows the decreased defect resistances for different combinations of field and defect sizes. Therefore, for the defect detected in Fig. 1(b), individual thermometer shows that defect pre-heating is 400~900mK (after taking into account the thermometer efficiency). From Fig. 8 and Table 1, actual defect size can be concluded as 40~120 μm and effective defect resistance is 0.5~2m Ω . Since the observed pit in Fig. 1(b) is much larger than this actual region responsible for quench, we conclude that only a small region of the observed pit is responsible. This is entirely consistent with the possibility that only a small region of the pit has features such as sharp edges with enhanced fields.

CONCLUSION

A calculation to establish relationship between defects pre-heating and defects size has been done. The observed pit is much larger than the actual region responsible for quench. The correlation between defects size and pre-heating temperature near the defect region at helium side can provide us useful information about the effective defect size and resistance.

REFERENCES

- [1] J. Knobloch, PhD thesis, Cornell University, 1997.
- [2] A. Romanenko, PhD thesis, Cornell University, 2008.
- [3] H. Padamsee et.al., “RF superconductivity for accelerators”, 1998.
- [4] Y. Iwashita et.al., “Development of high resolution camera and observations of superconducting cavities”, EPAC08, Genoa, Italy.
- [5] J. Wiener, H. Padamsee, “Thermal and statistical models for quench in superconducting cavities”, TESLA Report 2008-08.
- [6] A. Deniz, H. Padamsee, “A calculation of the radio-frequency thermal magnetic breakdown threshold for superconducting niobium”, CLAN-79/434,1979.